IR Structural Identification of Oxocumulene···HCl Complexes Generated in Cryogenic Matrixes. The Product-like Transition State of the Corresponding Electrophilic Addition

Nathalie Piétri, Thierry Chiavassa, Alain Allouche, and Jean-Pierre Aycard*

URA CNRS 773, Physique des Interactions Ioniques et Moléculaires, Équipe Spectrométrie et Dynamique Moléculaire, Université de Provence, Case 542, 13397 Marseille Cedex 20, France

Received: September 25, 1996; In Final Form: November 18, 1996[⊗]

The structure and energy properties of the 1:1 complex formed between HCl and carbon suboxide C_3O_2 (**3**) have been investigated using FTIR matrix isolation spectroscopy and ab initio calculations at the MP2/6-31G** level. Investigations have been extended to other oxocumulenes such as $H_2C{=}C{=}O$ (**1**), and $(CH_2)_2$-CCO (**2**) complexed by HCl. Trapped in argon matrixes, these complexes are characterized by a large shift of the ν_{HCl} stretching mode to lower frequencies (191, 135, and 150.5 cm^{-1} for **1**−**3**, respectively). The similarity of IR spectra of the complexes generated in the gas or in the solid phase is indicative of a similar inclusion site. Concordance between experimental and calculated ν_{HCl} shifts is obtained with T-shaped complexes. These complexes describe the interaction between hydrogen and the C_β carbon atom of the ketene moiety. The geometrical modifications of the ketene subunit suggest that the complex is the product-like transition state of the corresponding electrophilic addition to the carbon atom.

Introduction

The structure and potential energy surfaces of weakly bonded molecular complexes are the subject of much current experimental and theoretical study. Complexes in which the components interact through a hydrogen bond have attracted special interest,[1−4] especially the complexes between hydrogen halides and a variety of molecules (including very weak bases such as CO_2 or CO). This field has been extensively studied using molecular beams, rotational spectroscopy,[1g,i−l] ab initio calculations,[1a,d,b] and matrix isolation techniques.[1f,g,k,q,n,2−4]

A large part of this work has focused on the development of cryogenic techniques for the production of complexes and on the determination of their high-resolution infrared spectra. The sample is generally obtained by depositing or co-depositing of the gas mixture (diluted in an inert gas) on a window cooled to 20 K. Certain recent results present a noncomplicated experimental technique that consists in trapping a gas-phase mixture (i.e., aggregation, surface diffusion during deposit, etc.). In such an approach, the complexes are obtained by photodecomposition of a precursor trapped in a low-temperature matrix.[2−4] The photoproducts formed under UV irradiation are trapped in this matrix, and the cage effect prevents the photofragments from leaving the original site. This approach was used successfully to produce and identify FH···CO,[2] HCOOH···CO,[3a] H_2O···CO,[3b] $(CH_2)_2$CCO···HCl,[5a] and $H_2C{=}C{=}O$···HBr[4b] and ···HCl[4a] hydrogen-bonded complexes.

The results for 1:1 molecular complexes between ketene derivatives and HCl were obtained in earlier work at our laboratory.[5] As was observed by Kogure et al.,[4] these complexes are characterized by a significant shift of the fundamental vibrational frequency of HCl to a lower frequency (see Table 1). The purpose of the present work is to obtain direct and accurate results allowing the geometries of certain oxocumulene···HCl 1:1 complexes to be determined. The oxocumulenes studied in this work with atoms numbering are reported in Figure 1. Acyl chloride derivatives were isolated in rare-gas matrixes[4a,5] and then UV photolyzed. Quantum calculations were performed to determine the **L** and **T** complex structures and to compare the experimental IR spectra with the calculated spectra.

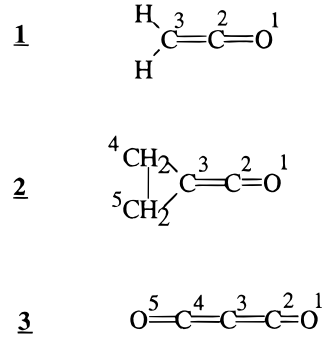

Figure 1. Structure of the oxocumulene compounds and numbering of the atoms.

Experimental Method

The infrared spectra were measured of the **1**···HCl,[4a] the **2**···HCl,[5a] and the **3**···HCl[5b] molecular complexes obtained by UV photolysis of acetyl chloride,[4a] cyclopropyl acid chloride,[5a] and chloroformylketene,[5b] respectively. These spectra have been described in earlier works.

HCl was supplied by the Matheson Co. Pure C_3O_2 was synthesized using the method described by Miller et al.[6] C_3O_2 and HCl were distilled from trap-to-trap on a vacuum line before use.

The apparatus and experimental techniques used to obtain the pure C_3O_2 and C_3O_2/HCl argon matrixes have been described in other works.[7] The relative concentration of rare gas to C_3O_2 or C_3O_2/HCl at room temperature (M/S ratio) was adjusted on the basis of pressure measurements. The mixture was deposited at 20 K on a CsBr window. The rate of gas mixture was controlled using an Air Liquide microleak (V.P/RX). This rate ($\leq$2 mmol/h) was chosen to prevent as much site splitting of the vibrational absorption bands as possible.

The IR spectra were recorded at 15 K in the 400−4000 cm^{-1} region on a 7199 Nicolet spectrometer equipped with a N_2-cooled MCT detector. The resolution was 0.12 cm^{-1} without apodization.

[⊗] Abstract published in *Advance ACS Abstracts,* January 1, 1997.

S1089-5639(96)02953-2 CCC: $14.00

TABLE 1: Experimental and Calculated ν_{HCl} and ν_{CCO} Frequency Shifts (cm^{-1}) in Oxocumulene···HCl Complexes ($\Delta\nu = \nu_{isolated} - \nu_{complexed}$, Values in Subcript Are the References Numbers)

	ν (cm^{-1})					$\Delta\nu$ (cm^{-1}		
	experiment		calculated				calculated	
				complexed				
base	isolated	complexed	isolated	**L**	**T**	experiment	**L**	**T**
				ν_{HCl}((R0+P1)/2)				
none	2870		3119					
CO_2		2854[1h]		3014[1h]		17[1h]	21[1h]	
CO		2815[3]				55.5[3]		46.5[1b]
				3118	3064		1	55
1		2679[4a]		3073	2911	191[4a]	46	208
2		2735[5a]		3016	2510	135[5a]	103	609
3		2719.5[5b]		3101	2981	150.5[5b]	18	137
				ν_{CCO}				
CO	2139	2154[3]	2119	2117	2137	−15[3]	2	−18
1	2138	2137[4a]	2238	2236	2234	1[4a]	2	4
2	2176−2154	2145−2125[5a]	2282	2258	2214	30[4b]	24	68
3								
ν_s	2196	2194[5b]	2249	2253	2243	2[5b]	−4	6
ν_{as}	2289	2232[5b]	2485	2486	2377	49[5b]	−1	108

Results and Discussion

Chloroformylketene (Cl−CO−CH═C═O) was obtained from malonyl dichloride thermolysis in the gas phase; then, it was isolated in a rare-gas matrix. The rare-gas cages thus embedded a single molecule (chloroformylketene or HCl), and the complexes were excluded. The chloroformylketene molecules were then irradiated ($\lambda \geq 310$ nm) to obtain carbon suboxide **3** complexed by HCl.[5b] The absence of C_3O_2 monomer in Figure 2d shows that this compound generated by the photolysis of chloroformylketene in the argon matrix is trapped with HCl in the same cage, forming an 1:1 complex. After annealing at 30 K (Figure 2e), we observe the formation of C_3O_2 monomer. In this experiment, the broad absorption band characteristics of the ν_{HCl} stretching mode appeared at 2719.5 cm^{-1} (see Figure 2). This frequency is lower than the value observed for free HCl trapped in an argon matrix ($\Delta\nu = 150.5$ cm^{-1}). A similar frequency shift is observed for C_3O_2, which presents an absorption band at 2233 cm^{-1} with site splitting. When isolated in an argon matrix, the free molecule absorbs at 2289 cm^{-1} (see Figure 2).

The spectra recorded after co-depositing of argon/C_3O_2 and argon/HCl samples at 15 K (see Figure 2) show only slight differences with respect to those obtained by photolysis of chloroformylketene. In the HCl region, the rovibrational structure of free HCl presents, below 2800 cm^{-1}, $(HCl)_n$ (n = 2, 3, ...) polymer absorption bands. The 2719.5 cm^{-1} frequency attributed to the HCl···C_3O_2 complex in the previous experiments[5b] is also observed with the corresponding 2233 cm^{-1} absorption (in the C_3O_2 frequency range) but without site splitting (see Figure 2).

HCl is formed complexed with **2** after photolysis at $\lambda \geq 230$ nm of cyclopropane carbonyl chloride ($(CH_2)_2CHCOCl$) isolated in rare-gas matrix at 15 K.[5a] Its stretching mode is shifted by 135 cm^{-1} (cf. Figure 4 in ref 5a) below the frequency of monomer HCl in rare-gas matrixes. The ν_{CCO} stretching mode of cyclopropylidene ketene **2** takes the form of a broad band between 2145 and 2125 cm^{-1}. This value is similar to those observed by Baxter[8a] and Wentrup[8b] (2145−2125 and 2154−2135 cm^{-1}, respectively), and it is slightly shifted with respect to those of pure **2** (2176−2154 cm^{-1}) obtained by Maïer[8c] by thermolyzing the 1-pyrazoline-3,5-dione derivative.

Using UV photolysis of acetyl chloride in an argon matrix, Watari and co-workers[4a] observed the ν_{CCO} stretching frequency of the ketene **1** at 2137 cm^{-1}. Except for slight frequency shifts, the spectra of **1** photoproduct are the same as those of free **1** in solid argon ($\nu_{CCO} = 2138$ cm^{-1}). The fundamental vibrational frequency of HCl in the complex is however observed at 2679 cm^{-1} (1939 cm^{-1} for DCl), i.e., 191 and 141 cm^{-1} below the frequencies of the free HCl and DCl in solid argon. To identify the formation of the complex, argon/ketene and argon/HCl (DCl) samples were co-deposited. Similar absorption bands were observed as well as absorption due to free HCl (DCl).

These latter results and those obtained for **3**···HCl complex, suggest that the structure for the complexes is identical whether obtained in the gas or the solid phase, i.e., the matrix is really an inert medium without interference in the photochemical process.

Comparison of the infrared data obtained in the present experiments and in previous works for CO,[1c,g] **3**,[5b] **2**,[5a] and **1**[4a] interacting with HCl shows a great resemblance between the vibrational properties of HCl (see Table 1). These results are quite different from those obtained for CO_2···HCl complex observed in the gas phase[1l] or in an argon matrix.[1k] In the latter case, the frequency of the HCl stretching mode is shifted to lower frequency with respect to the monomer vibrational frequency in argon ((R0 + P1)/2 line) by merely 17 cm^{-1}. Likewise, the CO_2 submolecule modes presents slight displacements toward both high and low frequencies (5 cm^{-1} for the ν_{as} stretching mode). The ν_{HCl} stretching mode for the **3**, **2**, **1** series and for the CO is shifted by 150.5, 135, 191, and 55.5 cm^{-1}, respectively. The latter value is obtained for the stable ClH···CO complex. For the tilted CO···HCl complex, lower values are to be expected,[1k] as was observed by Willner *et al.*[2] for the ν_{HF} in OC···HF and FH···OC complexes trapped in an argon matrix (130 and 12 cm^{-1}, respectively, with respect to the monomer ν_{HF} stretching mode). For the CO_2···HCl 1:1 complex, the linear structure was established[1k,1l] as was the CO_2···HF complex.[1a] These last examples show an important shift difference between C and O complexes.

Ab Initio Computation. *Computational Details.* To establish the molecular structures of the **1**, **2**, and **3** HCl complexes, ab initio calculations were carried out using Gaussian 94[9] at the MP2/6-31G** level.[10]

Several possible geometric arrangements are possible in the acid and base subunits in the complexes. The presence of the highest occupied molecular orbital perpendicular to the ketene plane, and the lowest unoccupied molecular orbital in the ketene plane place substantial negative charges on oxygen and on C_3.[11]

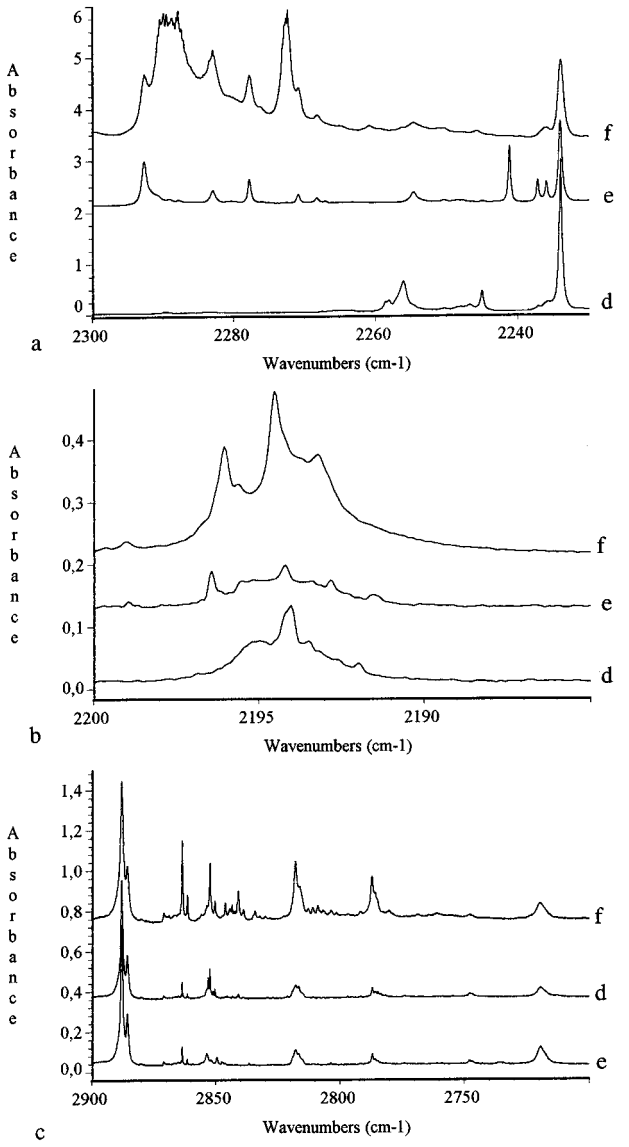

Figure 2. Infrared spectra of **3**···HCl complex and **3** isolated in an argon cryogenic matrix: (a) ν(C═C═O_{as}) range 2300−2210 cm^{-1}; (b) ν(C═C═O_s) range 2200−2188 cm^{-1}; (c) ν(H−Cl) range 2905−2698 cm^{-1}; (d) spectra obtained by photolysis of chloroformyl ketene; (e) spectra obtained by photolysis of chloroformylketene, after annealing at 30 K; (f) spectra obtained by co-depositing C_3O_2 and HCl.

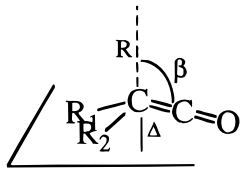

Figure 3. Pyramidalization of the ketene group.

SCHEME 1

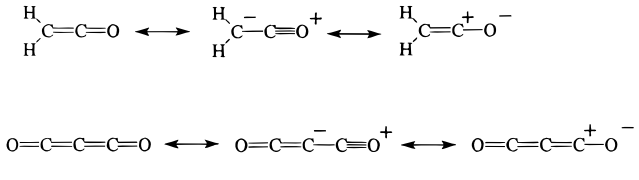

This corresponds to the expected resonance structures (see Scheme 1). Hence, the electrophiles are expected to attack the ketene perpendicular to the molecular plane at the two positions. Two kinds of complexes are thus considered for optimization and vibrational frequency calculations: the **L** form, which involves the hydrogen bonding with the terminal oxygen atom, and the **T** form, for which hydrogen bonding occurs with the C_3 carbon atom (see Scheme 2).

SCHEME 2

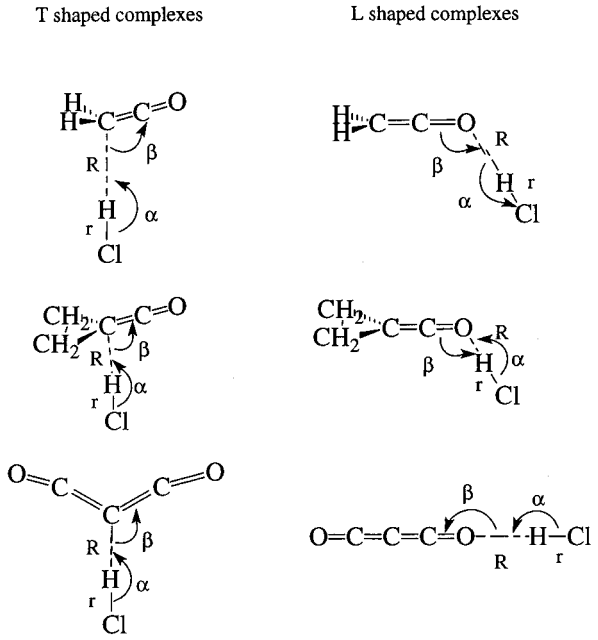

SCHEME 3

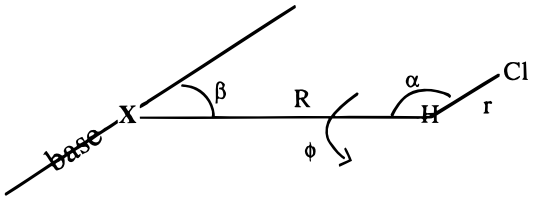

To determine the geometry of the complexes, two types of four-dimensional ground-state potential energy surfaces (PES) were explored using the three independent variables R, α, and β displayed in Scheme 3. R is the distance between the HCl hydrogen atom and an X atom (carbon or oxygen) of the base moiety. α is the intermolecular angle between R, and the molecular axis of HCl and β is the intermolecular angle between R and the ketene group of the base (see Scheme 3). In a first approximation, the "out-of-plane angle ϕ" (i.e., the dihedral angle between the base and HCl) was assumed to be 0° for **3** and 90° for **1** and **2**. Owing to computational constraints, it was not possible to optimize all the geometrical parameters for all points of the ground state. In the first approximation of the different values of R, the intermolecular angles α and β were varied, all the other intramolecular parameters were held constant at their MP2/6-31G** equilibrium values. The stabilization energy of the complex AB under study is evaluated by $\Delta E = E(\mathrm{AB}) - E^{\mathrm{BSSE}}(\mathrm{A}) - E^{\mathrm{BSSE}}(\mathrm{B})$ were E^{BSSE}(A) and E^{BSSE}(B) are the respective energies of the A and B moieties corrected from the basis set superposition error (BSSE) by the usual conterpoise methode.[12]

For the **L** (R = O···HCl) and **T** forms (R = C···HCl), four 3-D surfaces were carried out for R = 1.8, 2.0, 2.2, 2.5 Å. The number of points in α ranged from 90° to 270° in 30° steps, and from 90° to 180° in β. This type of surface is very flat, but the minimum energy was determined for each 4-D surface corresponding to **L** and **T** complexes.

Starting from these initial approximations, all the geometrical parameters were fully optimized (using the Berny optimization

TABLE 2: Geometrical Parameters (Lengths in Å, Angle in deg) and Energies (hartrees). Values of the Monomers and the Complexes (r_{12} and r_{23} Are the Internal Monomers Bonds)

					1···HCl		**2**···HCl		**3**···HCl	
	HCl	**1**	**2**	**3**	**L**	**T**	**L**	**T**	**L**	**T**
r_{12}		1.180	1.186	1.183	1.183	1.175	1.193	1.178	1.185	1.177
r_{23}		1.320	1.292	1.279	1.315	1.327	1.291	1.320	1.276	1.299
OCC		180	180	180	179.6	177.5	176.5	171.6	180.0	174.9
r	1.269				1.272	1.283	1.277	1.310	1.271	1.278
α					167.2	174.7	171.8	163.9	180	179.9
β					118.3	98.4	117.9	113.3	180	109.5
R					2.142	2.214	2.039	1.859	2.171	2.240
Δ		0	0	0	0	0.1	0	0.4	0	
E_h	−460.205 446	−152.163 341	−229.289 519	−264.006 572	−612.374 159	−612.375 01	−689.502 242	−689.507 403	−724.216 204	−724.215 460
$E_L - E_T$ (kcal/mol)					0.48		3.23		−0.46	

procedure). The harmonic vibrational frequencies were determined at the stationary points and compared to experimental data.

Geometries of the Monomer Oxocumulenes. Optimization of the geometrical parameters for the ground state of ketene **1** leads to a C_{2v} structure, with a C═C bond length of 1.318 Å and a C═O bond length of 1.179 Å. The CCO angle is 180° (see Table 2). This structure agrees quite well with experimentally determined values (1.315 and 1.16 Å, respectively[13]) and with previous theoretical results.[14]

The **2** singlet ground state is C_{2v} with C═C and C═O bond lengths of 1.187 and 1.292 Å, respectively. In accordance with previous results,[11,14] the CCO angle is equal to 180° (see Table 2).

Carbon suboxide **3** is a nearly linear molecule (i.e., the molecular system has a large floppy amplitude vibration[15,16]). Therefore, its geometry cannot be properly represented by a linear model or by a model bent about the central carbon atom. Although C_3O_2 is known to be bent from spectroscopic measurements,[14] it is usually treated as if it were linear.[17] The present ab initio calculation on C_3O_2 using an extended basis set (6-31G**) and Møller−Plesset second-order correction (MP2) led to a linear $D_{\infty h}$ structure (see Table 2).

Geometries of the HCl···Oxocumulene Complexes. ***1*···*HCl:*** The **L** ketene···HCl complex calculation gives a local minimum for $\phi = 0,°$ $R = 2.146$ Å, and α and $\beta = 180°$. The subsequent variation of ϕ between 0° and 180° gives a stationary point for $R = 2.142$ Å, $\phi = 90°$, $\beta = 118.3°$, and $\alpha = 167.2°$ with a variation of energy about 0.39 kcal mol^{-1}, which confirm the validity of our approximation (see Table 2). When the hydrogen atom interacts with the carbon atom (**T** complex), the energy decreases. Its value and the other optimized parameters are given in Table 2. The H−Cl distance with respect to monomer molecule is greater (by 0.01 Å) in the **T** form than in the **L** form. The **T**-shaped form is slightly more stable, but the energy difference (0.48 kcal mol^{-1}) is not significant at this level of theory; it can thus be considered as equivalent. After BSSE correction had been carried out by the counterpoise procedure,[12] the **T** and **L** complexes are stabilized with regard to monomer molecule by 2.33 and 2.24 kcal mol^{-1}, respectively.

2*···*HCl: After complete optimization of the different parameters (R, α, β, ϕ), unlike that observed for the **1**···HCl and **3**···HCl complexes, the **T** structure is largely stabilized with regard to the **L** structure (3.23 kcal mol^{-1}). Moreover, the **T** and **L** complexes are stabilized in respect to monomer molecule by 4.98 and 3.12 kcal mol^{-1}. For **L** and **T** forms, the HCl distances are greater than the values calculated in the isolated molecule and in **1**···HCl and **3**···HCl complexes. What is more, the R distance is shorter than that observed in the other **L** and **T** complexes. The optimized parameters are given in Table 2.

3*···*HCl: First, the **L** complex (interaction between hydrogen of HCl and the terminal oxygen atom) is assessed. The minimum energy, in the 4-D hypersurface is obtained for $R = 2.2$ Å, where α and β are equal to 180° (see **L** in Scheme 2). After complete optimization of the geometrical parameters, α and β remain equal to 180° and R undergoes a very slight change (0.03 Å).

For the **T**-shaped structure, the 4-D PES gives a stationary point for $R = 2.2$ Å, $\alpha = 180°$, and $\beta = 105°$. The optimized parameters, given in Table 2, show that in the **T** complex, the carbon suboxide is bent at the central carbon atom with an equilibrium CCC bond angle of 142°, while the **L** complex remains linear.

As with the **1**···HCl complex, the H−Cl distance with respect to the free molecule is greater for the **T** form than for the **L** form. These distances were equal to 1.278 and 1.271 Å, respectively. On the other hand, the **L** complex is more stable (by 0.46 kcal mol^{-1}) than the **T** complex, but this difference is not very significant in determining clearly the structure present in cryogenic matrixes. The **T** and **L** structures are stabilized in respect with the monomer molecules by 0.65 and 1.76 kcal mol^{-1}, respectively.

Identification of the Complexes. The preceding calculation provides valuable insight into the stability and the spectroscopic features of the complexes. First, the complexation effects can be observed on the geometry of the partner molecules and on their most significant stretching frequencies

Analysis of Table 2 data shows certain differences between the geometrical parameters of the complex moieties with regard to those of the free molecules.

Except for the **2**···HCl complex, for which the **T** structure is largely stabilized with respect to the **L** form. The difference in energy E(**L**) − E(**T**) for **1**−**3** is 0.48, 3.23, and −0.46 kcal mol^{-1}, respectively. It must be kept in mind that the perturbation of the system due to the crystal matrix potential is not exactly known, but it is certainly at least of the same order of magnitude as the energy difference between the **L** and **T** structures. To identify the form present in argon matrixes, we must compare the ν_{HCl} vibrational frequency shift of the two complexes with regard to the calculated ν_{HCl} of the free HCl (3119 cm^{-1} corresponding to ν(R0+P1)/2 lines).

For the **2**···HCl complexes, the calculated shifts are much greater (103 and 609 cm^{-1} for the **L** and **T** structures, respectively) than those obtained for the other complexes. We have established that, for these complexes, the geometrical parameters (Table 2) are surprisingly different, the length of r (H−Cl bond, cf. Scheme 3) is overestimated, and R is underestimated.

The respective contributions of R and r to the total energy of the system were then analyzed. All optimized parameters were held constant except R, which varied from 1.7 to 2.4 Å in 0.1 Å steps. The three energy curves obtained for $r = 1.27$, 1.28, and 1.29 Å are reported in Figure 4. These curves are very flat

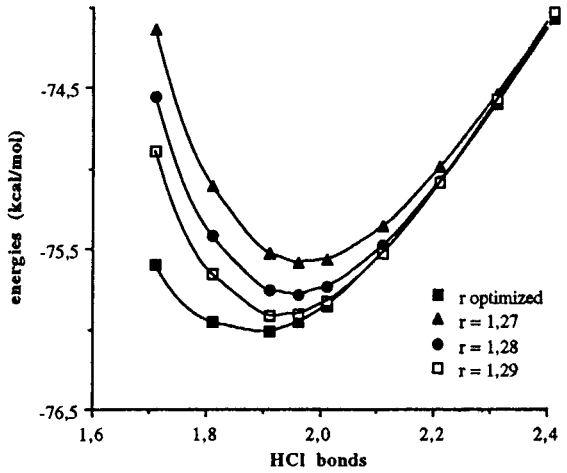

Figure 4. Energy curves for $R = 1.95$ Å. The HCl distance is given in angstroms, and the energies in kcal mol^{-1}.

and show a minimum R value of 1.95 Å. A large variation in r ($\Delta r = 0.1$ Å) induces a slight decrease in the energy (0.5 kcal mol^{-1}).

For the **L** complex, only $R = 1.95$ Å and $r = 1.27$ Å were considered, using the average values obtained for the **1** and **3** complexes and the $\Delta\nu_{HCl}$ shifts from 103 to 42 cm^{-1}. Likewise, for the **T** complex, when $R = 1.95$ Å and $r = 1.28$ Å, this shift becomes equal to 289 cm^{-1}. It has been established that a weak variation of energy produces a significant change in the frequency shift, since the potential curves are very flat.

The geometrical parameters of the **T** complex (Table 2) indicate that it is much more compact than the other complexes. This is most probably the result of the well-known stabilization of the three-membered ring when its functional carbon atom evolves from sp^2 to sp^3 hybridization. Turro and Hammond[18] indeed observed that an exocyclic double bond to a three-membered ring confers high reactivity as a result of the internal strain.[19] On the other hand, the low rate of solvolytic displacement for cyclopropyl tosylates indicates that the formation of cyclopropyl cation requires a high activation energy level.

In the case of the **3**···HCl complex, the calculated ν_{HCl} stretching mode is shifted by 18 and 137 cm^{-1} for the **L** and **T** structures, respectively (see Table 1). In the **1**···HCl complex, this value is shifted by 46 and 208 cm^{-1} for the **L**- and **T**-shaped complexes, respectively.

For the HCl moiety, a slight lengthening of the bond lengths (see Table 2) is observed in the **L** complexes ($0.001 \leq \Delta r \leq 0.003$ Å). In the **T**-shaped structures, these differences are greater ($0.008 \leq \Delta r \leq 0.015$ Å) and can be correlated to the large ν_{HCl} shift observed experimentally (see Table 1).

These results are compatible with the **T**-shaped structures of the complexes, which are indicative of hydrogen bonding with the C_β carbon atom of the ketene function. For **3**···HCl, this result is similar to those obtained by Tortajada et al.[20,21] using FT ion cyclotron resonance and ab initio calculations for the $C_3O_2H^+$ species.

For the base subunits, two types of modifications are observed:

(1) The r_{12} bonds between the O_1 and C_2 atom of the ketene moieties (cf. Figure 1) are unperturbed for **L** complexes ($\Delta r \approx 0.001$ Å) and they are slightly shortened for **T** complexes ($0.005 \leq \Delta r \leq 0.013$ Å). On the other hand, the r_{23} bonds between C_2 and C_3 atoms of the ketene moieties are shortened (0.004 Å) and lengthened ($\Delta r \approx 0.013$ Å) in the **L** and **T** complexes respectively.

(2) Pyramidalization occurs at the C_3 carbon in the **T** complexes (see Figure 3).

The experimental and calculated ν_{CCO} frequency shifts of the complexed oxocumulenes are reported in Table 1. Examination of the data shows that the calculated ν_{CCO} stretching frequency shifts coincide with the experimental values for the **T** structure. For **3**···HCl, the shift for the unscaled frequency is 108 cm^{-1}.

As with the analysis of nucleophile−electrophile interactions in crystal packings,[22] **1** and **2** calculation results of the donor−acceptor interactions can be analyzed in terms of geometrical parameters: the distance R ($H^+\cdots C_3$) between the reactant electrophilic atom and the nucleophilic carbon C_3, the angle β (HCC), and the pyramid height Δ between the top C_3 carbon and the base consisting of the C_2 and the two other atoms covalently bonded to the C_3 carbon (see Figure 3).

The electrophilic reagent H^+ approaches the C_3 carbon atom in the bisector plane at an angle β greater than 90°. The degrees of pyramidalization Δ are close together. These observations suggest a product-like transition state for a mechanism involving direct protonation on the central carbon. This mechanism is different from those observed by Satchell,[23] in which the addition of hydrogen halides to ketene derivatives involved carbonyl addition, and subsequent catalyzed prototropy from an unobserved enol intermediate. This mechanism is corroborated by the mechanistic results of Allen et al. for the hydration of ketenes[24] and carbon suboxide.[25] In this last experiment, the authors[25] observed a linear dependence of the rate on [H^+] and an isotopic effect consistent with a mechanism involving rate-limiting proton transfer to the central carbon.

Conclusion

The present study is devoted to the formation and the structural determination of 1:1 complexes of carbon suboxide (and other oxocumulenes) with HCl. The results accomplished from theoretical calculations strongly suggest that, after photolysis in a low-temperature matrix gas, the bimolecular reaction between the partners produces stable complexes. The similarity of the IR spectra of the complexes formed in the gas, or complexes photosynthesized in the solid phase, is indicative of an absence of specific matrix effects of the matrix during its formation. Distinct shifts were observed in the vibrational modes of both the acid and base subunits in the complex. The magnitude of ν_{HCl} shift is characteristic of **T**-shaped complexes, which implies hydrogen bonding with the C_β carbon atom of the ketene function. The structural modifications of the complex's ketene moiety suggest that the corresponding electrophilic addition to central carbon involves a product-like transition state.

Acknowledgment. The CNRS (IDRIS) are gratefully acknowledged for their financial support. We thank Professors H. Bodot and J. Pourcin for their invaluable remarks.

References and Notes

(1) (a) Sadlej, J.; Roos, B. O. *Theor. Chim. Acta* **1989**, *73*, 173. (b) Bacskay, G. B. *Mol. Phys.* **1992**, *77*, 61. (c) Mc Kellar, A. R. W.; Lu, Z. *J. Mol. Spectrosc.* **1993**, *161*, 542. (d) De Almeida, W. B. *Chem. Phys. Lett.* **1990**, *166*, 589. (e) Barnes, A. J. *J. Mol. Struct.* **1983**, *100*, 259. (f) Barnes, A. J.; Lasson, E.; Nielsen, C. J. *J. Chem. Soc., Faraday Trans.* **1995**, *91*, 3111. (g) Soper, P. D.; Legon, A. C.; Flygare, W. H. *J. Chem. Phys.* **1981**, *74*, 2138. (h) Legon, A. C. Millen, D. J. *Chem. Soc. Rev.* **1992**, *21*, 71. (i) Legon, A. C.; *Chem. Sov. Rev.* **1990**, *19*, 197. (j) Legon, A. C.; *Chem. Commun*. **1996**, 109. (h) Fourati, N.; Silvi, B.; Perchard, J. P. *J. Chem. Phys.* **1984**, *81*, 4737. (k) Altman, R. S.; Marshall, M. D.; Klemperer, W. *J. Chem. Phys.* **1982**, *77*, 4344. (l) Zeegers-Huyskens, T. *J. Mol. Struct.* **1993**, *297*, 149. (m) De Almeida, W. B.; Hinchiffe, A. *Chem. Phys.* **1989**, *157*, 143. (n) Baiocchi, F. A.; Dixon, T. A.; Joyner, C. H.; Klemperer, W. *J. Chem. Phys*. **1981**, *74*, 654. (o) Andrews, L.; Johnson, G. L. *J. Chem. Phys*. **1982**, *76*, 2875. (p) Bach, S. B.; Ault, B. S. *J. Phys. Chem.* **1984**, *88*,

3600. (q) Perchard, J. P.; Cipriani, J.; Silvi, B.; Maillard, D. *J. Mol. Struct.* **1982**, *100*, 317.

(2) Schatte, G.; Willner, H.; Hoge, D.; Knözinger, E.; Schrems, O. *J. Phys. Chem.* **1989**, *93*, 6025.

(3) (a) Lundell, J.; Räsänen, M. *J. Phys. Chem.* **1993**, *97*, 9657. (b) Lundell, J.; Räsänen, M. *J. Phys. Chem.* **1995**, *99*, 14301.

(4) (a) Kogure, N.; Ono, T.; Suzuki, E.; Watari, F. *J. Mol. Struct.* **1993**, *296*, 1. (b) Kogure, N.; Hatakeyama, R.; Suzuki, E.; Watari, F. *J. Mol. Struct.* **1993**, *299*, 105.

(5) (a) Monnier, M.; Allouche, A.; Verlaque, P.; Aycard, J. P. *J. Phys. Chem.* **1995**, *99*, 5977. (b) Piétri, N.; Chiavassa, T.; Allouche, A.; Rajzman, M.; Aycard, J. P. *J. Phys. Chem.* **1996**, *100*, 7034.

(6) Miller, F. A.; Fateley, W. G. *Spectrochim. Acta* **1964**, *20*, 253.

(7) Monnier, M. Photoisomerisation et Photolyses en matrixes cryogeniques: identification des entités moléculaires et suivi cinétique par IR-TF. D.Sc. Thesis, Université de Provence, Marseille, 1991.

(8) (a) Baxter, G. J.; Brown, R. F. C.; Eastwood, F. W.; Harrington, K. J. *Tetrahedron Lett.* **1975**, 4283. (b) Leung-Toung, R.; Wentup, C. *J. Org. Chem.* **1992**, *57*, 4850. (c) Maïer, G.; Heider, M.; Sierakowski, C. *Tetrahedron Lett.* **1991**, *32*, 4850.

(9) Gaussian 94, Revision C.2; Frisch, M. J.; Trucks, G. W.; Schlegel, H. B.; Gill P. M. W.; Johnson, B. G.; Robb, M. A.; Cheeseman, J. R.; Keith, T.; Petersson, G. A.; Montgomery, J. A.; Raghavachari, K.; Al-Laham, M. A.; G. Zakrzewski, V.; Ortiz, J. V.; Foresman, J. B.; Cioslowski, J.; Stefanov, B. B.; Nanayakkara, A.; Challacombe, M.; Peng, C. Y.; Ayala, P. Y; Chen, W.; Wong, M. W.; Andres, J. L.; Replogle, E. S.; Gomperts, R.; Martin, R. L.; Fox, D. J.; Binkley, J. S.; Defrees, D. J.; Baker, J.; Stewart, J. P.; Head-Gordon, M.; Gonzalez, C.; and Pople, J. A. Gaussian, Inc., Pittsburgh, PA, 1995.

(10) (a) Hehre, W.J.; Ditchfield, R.; Pople, J. A. *J. Chem. Phys.* **1972**, *56*, 2257. (b) Hariharan, P. C.; Pople, J. A. *Theor. Chim. Acta* **1973**, *28*, 213. (c) Iordon, M. S. *Chem. Phys. Lett.* **1980**, *76*, 163.

(11) (a) Tidwell, T. T. In *Ketenes*; John Wiley & Sons: New York, 1994; pp 4−32 and refences therein. (b) Jorgensen, W. L.; Salem, L. In *The Organic Chemist's Book of Orbitals*; Academic Press: New York, 1973.

(12) Boys, S.; Bernardi, F. *Mol. Phys.* **1970**, *19*, 553.

(13) Herzberg, G. In *Electronic Spectra of Polyatomic Molecules*; Van Nostrand: Princeton, 1966.

(14) (a) Del Bene, J. E. *J. Am. Chem. Soc.* **1972**, *94*, 3713. (b) Mc Allister, M. A.; Tidwell, T. T. *Can. J. Chem.* **1994**, *72*, 882.

(15) (a) Auwera, J. V.; Johns, J. V. C.; Poliansky, O. L. *J. Chem. Phys.* **1991**, *95*, 2299. (b) Trinquier, G.; Malrieu, J. P. *J. Am. Chem. Soc.* **1987**, *109*, 5303. (c) Durig, J. R.; Kalasinsky, V. F. *J. Mol. Struct.* **1978**, *46*, 1. (d) Lozes, R. L.; Sabin, J. R.; Oddershede, J. *J. Mol. Spectrosc.* **1981**, *86*, 357. (e) Duckett, J. A.; Mills, I. M.; Robiette, A. G. *J. Mol. Spectrosc.* **1976**, *63*, 249.

(16) (a) Jensen, P. *J. Mol. Spectrosc.* **1984**, *104*, 59. (b) Jensen, P.; Johns, J. W. L. *J. Mol. Spectrosc.* **1986**, *106*, 118.

(17) Stout, J. M.; Dysktra, C. E. *J. Am. Chem. Soc.* **1995**, *117*, 5127.

(18) Turro, N. J.; Hammond, W. B. *J. Am. Chem. Soc.* **1967**, *89*, 1028.

(19) March, J. In *Advanced Organic Chemistry*, 3rd ed.; John Wiley & Sons: New York, 1985.

(20) Tortajada, J.; Provot, G.; Morizur, J. P.; Gal, J. F.; Maria, P. C.; Flammang, R.; Govaert, Y. *Int. J. Mass. Spectrom. Ion Processes* **1995**, *141*, 241.

(21) Provot, G. In *Complexes ion-neutre: espèces intermédiaires dans les décompositions de cations radicaux et cations organiques en phase gazeuse.* Thesis, Université Pierre et Marie Curie, Paris, 1993.

(22) (a) Cossu, M.; Bachmann, C.; N'Guessan, T. Y.; Viani, R.; Lapasset, J.; Aycard, J. P.; Bodot, H. *J. Org. Chem.* **1987**, *52*, 5313. (b) Bürgi, H. B.; Dunitz, J. D.; Schefter, E. *J. Am. Chem. Soc.* **1973**, *95*, 5065. (c) Bürgi, H. B.; Lehn, J. M.; Wipff, G. *J. Am. Chem. Soc.* **1974**, *96*, 1956.

(23) (a) Lillford, P. J.; Satchell, D. P. N. *J. Chem. Soc. B*, **1968**, 897. (b) Satchell, D. P. N.; Satchell, R. S. *Chem. Soc. Rev.* **1975**, *4*, 231. (c) See ref 19.

(24) (a) Allen, A. D.; Tidwell, T. T. *J. Am. Chem. Soc.* **1987**, *109*, 2774. (b) See ref 10a, p 623.

(25) Allen, A. D.; McAllister, M. A.; Tidwell, T. T. *J. Chem. Soc., Chem. Commun.* **1995**, 2547.